

Photo-oxidation by laser pulse induced desorption of phthalocyanines

M. Holz^a, J. Wichmann^a, R. Mitrić^b, L. Wöste^a, A. Lindinger^{a,*}

^aFreie Universität Berlin, Institut für Experimentalphysik, Arnimallee 14, DE-14195 Berlin

^bFreie Universität Berlin, Institut für Theoretische Physik, Arnimallee 14, DE-14195 Berlin

Abstract

Photo-oxidation of iron(II)-phthalocyanine (PcFe) has been observed in matrix assisted laser desorption/ionization (MALDI) and laser desorption/ionization (LDI) and is interpreted by theoretical molecular dynamics simulations. The two ionization methods show different amounts of μ -oxo-bridged PcFe-dimer and deliver evidence that MALDI produces less mechanical stress on the analyte. The typical proton-transfer in the MALDI-process does not occur which leads to the assumption of a released electron of the delocalized π -system.

© 2011 Published by Elsevier Ltd.

Keywords: MALDI, LDI, Phthalocyanine

1. Introduction

In the today's world phthalocyanines and their derivatives are widespread. Mainly used as dyes, they are also found in electronics, photo-dynamic therapy or modern optical devices. These manifold applications and their special physical and chemical properties have not only lead to numerous investigations on their optical, magnetic, and electric characteristics, but make them also very attractive in various research areas like crystallization and the usability as catalysts for O₂ reduction in biological fuel cell applications or as molecular switches.[1, 2, 3, 4, 5] Most of the experimental studies have been performed in solution or in solid form. Nevertheless they are simply brought into the gas phase by laser pulse irradiation due to the high absorbance of light in the visible and near UV wavelength regime.[6] Therefore, Pcs are suitable matrix substances for matrix-assisted laser desorption/ionization (MALDI).

Phthalocyanines are π -conjugated macro-cyclic ligands and can coordinate metal elements like iron to so called metal phthalocyanines (PcMs). Some of them show the ability to adapt an oxygen atom if the present partial pressure of oxygen is high enough.[7] In the case of iron(II)-phthalocyanine (PcFe), several studies suggest that the additional oxygen atom binds to the central iron atom.[8]

This work reports about PcFe and its transformation into the gas phase via MALDI and laser desorption/ionization (LDI). Whereas in LDI the substance is directly excited, in MALDI the energy of the laser pulse is mostly absorbed by the matrix substance and transfers part of that energy to the analyte. The indirect

*Corresponding author

Email address: albrecht.lindinger@fu-berlin.de (A. Lindinger)

18 energy transport has the advantage that the method can bring large fragile bio-molecules into the gas phase.
19 In most cases, the matrix substances are organic acids and provide a proton to a basic residue of the analyte.
20 In addition to the experimental results, molecular dynamics simulations have been utilized to support the
21 interpretation of the presented data.

22 2. Experimental

23 All experiments have been performed with a commercial Bruker MALDI mass spectrometer (Reflex,
24 Bruker Daltonics, Bremen, Germany). A short modification in the optical setup containing a dielectric mir-
25 ror in the beam path has been made, which allows to irradiate the sample either with the built-in nitrogen
26 laser (VSL-337ND, LSI) or ultra short laser pulses. The femtosecond laser setup (Kapteyn-Murmane De-
27 sign; Odin, Quantronix, Darmstadt) provides 70 fs laser pulses up to a pulse energy of $E = 1$ mJ at a central
28 wavelength of $\lambda_c = 800$ nm. A detailed description can be found elsewhere.[9] The advantage of femtosec-
29 ond laser pulses lies in the well defined beam profile and lower pulse-to-pulse deviation compared to the
30 nitrogen laser.

31 For LDI-measurements, 50 mg/ml PcFe were solvated in a mixture of acetonitrile and water (3:2) and stirred
32 for 30 minutes. $2 \mu\text{l}$ of this mixture has been placed on each spot of the sample holder, dried with a heat gun
33 for 15 minutes and cooled down below a fume hood for one hour. For MALDI-measurements 50 mg/ml of
34 each α -cyano-cinammic-acid and sinapinic acid has been dissolved in a mixture of acetonitrile and water
35 (3:2) and $0.1 \mu\text{l}$ trifluoroacetic acid. The PcFe solution as described in the previous paragraph was again
36 diluted in acetonitrile/water (3:2) in a ratio of 1:100, mixed with the matrix solution (1:1) and placed on
37 the sample holder. The process of drying is the same as explained for LDI. The phthalocyanine substance
38 was purchased from Alpha Aesar (Ward Hill MA, USA), all other chemicals have been ordered from Fluka
39 (Buchs, Switzerland).

40 3. Theoretical Methods

41 The molecular structure has been calculated using an annealing procedure combined with molecular
42 dynamics simulations at the semi-empirical AM1 level of theory.[10] The electronic structure was calcu-
43 lated with the MOPAC program package while the MD-simulation was performed with an in-house suite of
44 programs.[11]

45 The simulations were started at a temperature $T = 1000$ K and the system has been exponentially cooled
46 down to $T = 0$ K within 10 ps of simulation time. The step size was chosen in the range of molecular vibra-
47 tions to 1 fs. For a good statistics all structures have been carried out by varying the simulation parameters
48 such as initial structure and temperature, as well as cooling time of the system.

49 The obtained results from this annealing procedure have been further optimized using DFT. For this purpose
50 the ORCA-package has been used and the gradient corrected BP3LYP functional together with split valence
51 plus polarization (SVP) basis sets for H and C and the triple-zeta valence plus polarization (TZVP) basis
52 sets for Fe, N and O have been applied. To estimate proton affinities, the basis set has been extended to
53 double-zeta (DZ) for H and N. [12, 13, 14, 15]

54 4. Results and Discussion

55 4.1. MALDI and LDI of [PcFe]

56 All MALDI and LDI measurements were performed in positive ion mode. The MALDI mass spectrum
57 in fig. 1 shows the typical pattern: Fragments of the analyte mixed with fragments of the matrix and cluster
58 thereof at lower m/z -values and the analyte peak of PcFe at $m/z=568$. According to general MALDI mass
59 spectra one would expect a protonated and maybe some cationized species. The exclusive occurrence of
60 $[\text{PcFe}]^+$ suggests only a minor influence to charge transfer of the matrix substance. The observed side peaks
61 in the mass spectrum reflect the isotopic abundances. In table 1 calculated proton affinities for different
62 attacking sites on PcFe are listed. Following expression (2) in Ref. [16], the change of the molar enthalpy

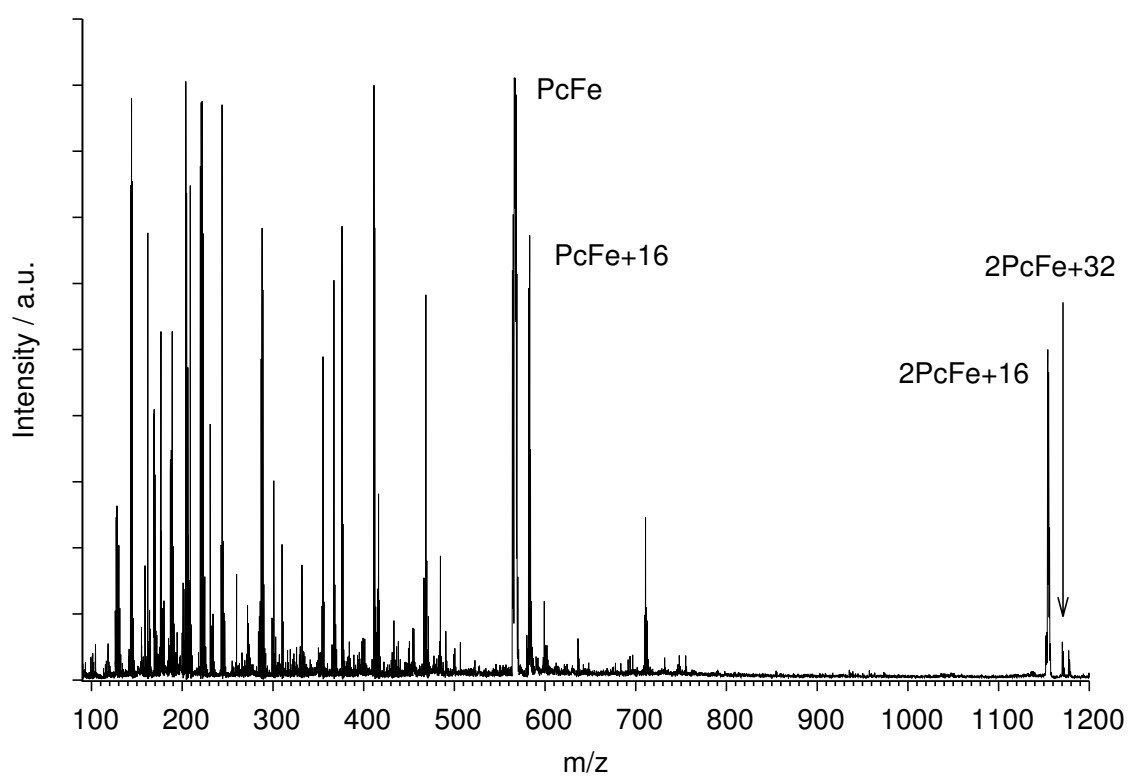


Fig. 1. MALDI mass spectrum of PcFe obtained with a pulse energy of $E = 2 \mu\text{J}$: Clusters and fragments are caused by the matrix in the lower mass region. The analyte peak is found at 568 u next to the oxidized species. At 1152 u the μ -oxo bridged dimer can be found together with a doubly oxidized dimer at 1168 u.

Protonated atom	ΔE_{el}^0	ΔE_{ZPE}	ΔH_{298}
N5	-169.7	8.3	-170.0
C1	-219.0	7.5	-213.0
C4	-185.8	7.1	-180.2

Table 1. Energetic quantities for calculating the proton affinities of PcFe for different attacking sites. All values are given in kcal/mol. See fig.3 for labeling.

63 for the reaction $[\text{PcFe}] + \text{H}^+ \rightarrow [\text{PcFe} + \text{H}]^+$ is given by $\Delta H_{298} = \Delta E_{\text{el}}^0 + \Delta E_{\text{ZPE}} + \Delta E_{\text{vib}} - \frac{5}{2}RT$. The first term,
 64 the difference in electronic energy ΔE_{el}^0 of reactants and product, is obtained by geometry optimizations.
 65 The change in energy associated with internal vibrations is the sum of the zero point energy ΔE_{ZPE} and a
 66 correction term ΔE_{vib} . The latter accounts for a redistribution of the vibrational population as a function
 67 of temperature. Assuming that $\Delta E_{\text{ZPE}} \gg \Delta E_{\text{vib}}$, it has been neglected. The estimated proton affinities
 68 range from $\text{PA}(\text{PcFe}) = 170$ kcal/mol to 213 kcal/mol. These are relatively high values and a proton transfer
 69 reaction from the matrix to $[\text{PcFe}]$ should be favorable. On the other hand, a delocalized electron of the
 70 π -system of the PcFe molecule can be easily detached by laser irradiation.

71 In the LDI mass spectrum (fig. 2) there are significantly less mass peaks in the low m/z range. The lack of
 72 peaks (up to $m/z = 450$) resulting from the matrix makes the identification of the parent and its corresponding
 73 fragments or clusters much easier. In this case one can identify three additional mass peaks, next to the
 74 parent ion, which are also visible in the MALDI mass spectrum. They are found at 584, 1152 and 1168 u.
 75 The first one has a shift of +16 mass units with respect to the analyte and suggests an attachment of either
 76 oxygen or a $-\text{NH}_2$ group. The latter can be excluded, because no stable structures could be obtained from
 77 the performed geometry optimization calculations. The other two observed mass peaks can be interpreted
 78 as a PcFe-dimer with a μ -oxo bridge between the two central iron atoms. The abundance of dimers is much
 79 higher in the MALDI spectrum which motivates the assumption of a soft release of the analyte into the
 80 gas phase. The matrix acts as a buffer and absorbs the kinetic energy of the molecules in the process of
 81 desorption. Moreover, other PcMs (PcCu, PcZn) have been investigated for oxygen attachment, but it has
 82 been solely observed with PcFe.

83 4.2. $[\text{PcFe}]^+$ and $[\text{PcFe}]-\text{O}^+$

84 In fig. 3 all successfully geometry optimized configurations with minimal energy are shown and obtained
 85 structural parameters are summarized in table 2. The electronic ground state of $[\text{PcFe}]^+$ is known as a $^4A_{2u}$
 86 open shell system.[17] The $[\text{PcFe}]^+$ cation (a) exhibits a flat planar structure with C_{2h} symmetry and is in
 87 agreement with recent theoretical results.[18] This optimized structure has been used as a basis for all further
 88 calculations.

89 The attachment of oxygen to $[\text{PcFe}]^+$ in (b) yields a distorted structure where the iron is displaced out of the
 90 plane, that is created by the nitrogen atoms of the pyrrole compounds, towards the oxygen, although the Pc
 91 configuration stays flat. In the accuracy of the calculation, the structure reveals a perfect D_{4v} symmetry.

92 4.3. $[2\text{PcFe}]^+ - \text{O}$ and $[2\text{PcFe}]^+ - \text{O}_2$

93 The dimer is formed in a reaction between a positively charged $\text{PcFe}^{(IV)}-\text{O}^+$ and a neutral $\text{PcFe}^{(III)}$,
 94 resulting in a $[\text{PcFe}^{(III)}-\text{O}-\text{PcFe}^{(III)}]^+$ -complex. Calculations of the μ -oxo diiron, fig.3 (c,d), lead to two
 95 different isomers. In structure (c) the iron atoms are coordinated in a square-pyramidal arrangement and the
 96 two phthalocyanines are rotated by 45° relative to one another. The Fe-O-Fe' bond shows a kink with an
 97 angle of $\theta_{\text{Fe}-\text{O}-\text{Fe}'} = 169.3^\circ$. The second conformer exhibits a parallel coordination of the PcFe-planes with
 98 an almost linear Fe-O-Fe' bond system of $\theta_{\text{Fe}-\text{O}-\text{Fe}'} = 178.8^\circ$. The other structural parameters of (c,e) are
 99 very similar. UV-vis, NMR, IR and Mössbauer experiments support the existence of two stable isomers, but
 100 so far no gas phase data is available.[19, 8] Furthermore, X-ray crystallographic analysis of μ -oxo diiron
 101 porphycene complexes data is present with Fe-O-Fe' angles of 178.7° and 145.3° and for μ -oxo-bis[(1-
 102 methylimidazole)-phthalocyaninatoiron(III)] of 175.1° . [20, 21] In both experiments rotated complexes are
 103 presented.

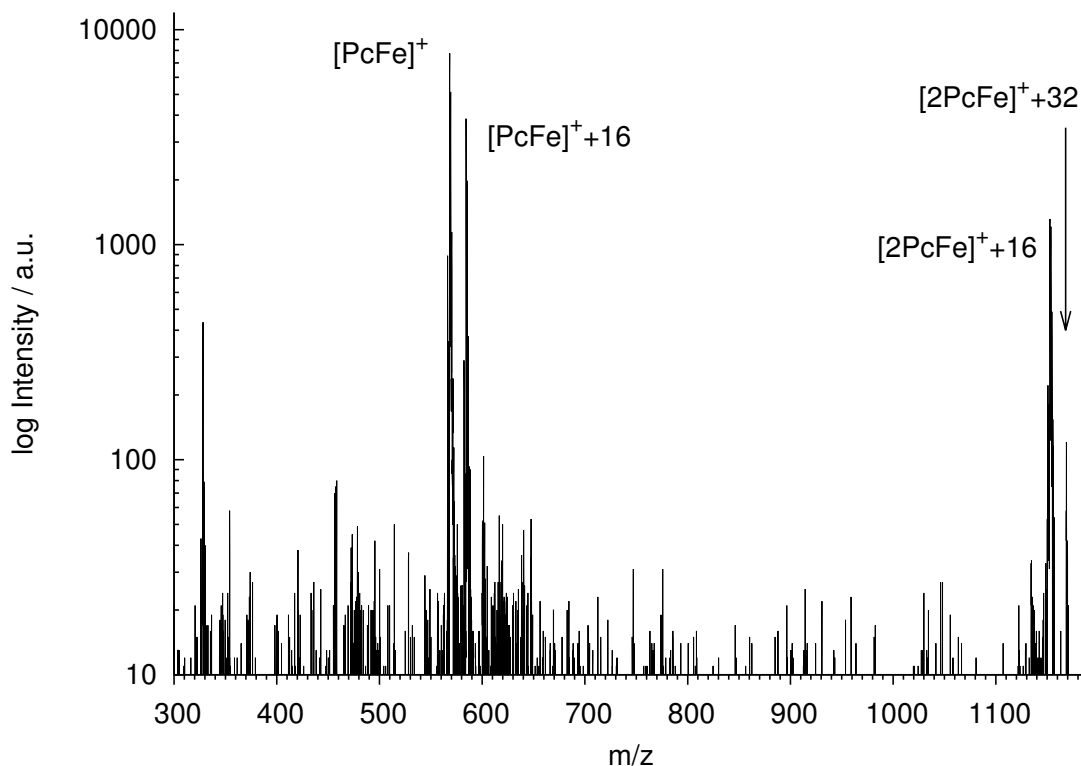


Fig. 2. LDI mass spectrum of PcFe obtained under the same conditions as the MALDI spectrum: At 568 u the ionized dye, the oxidized analyte at 584 u and the μ -oxo bridged dimer at 1152 u is visible. A mass peak with a low intensity at 1168 u which corresponds to two attached oxygen atoms can be observed.

	[PcFe] ⁺	[PcFe-O] ⁺	[2PcFe-O] ⁺ (c)	[2PcFe-O] ⁺ (e)	[2PcFe-O ₂] ⁺ (d)	[2PcFe-O ₂] ⁺ (f)
R_{N1-Fe}	1.944	1.962	1.983	1.983	1.988	1.981
R_{N2-Fe}	1.952	1.962	1.983	1.984	1.988	1.980
$R_{N1'-Fe'}$	-	-	1.982	1.983	1.970	1.979
$R_{N2'-Fe'}$	-	-	1.984	1.983	1.970	1.959
R_{Fe-O}	-	1.614	1.799	1.799	1.779	1.846
$R_{O-Fe'}$	-	-	1.798	1.801	1.955	1.747
$R_{Fe'-O'}$	-	-	-	-	1.658	1.813
$\theta_{N1-Fe-N3}$	180	163.3	160.0	159.7	158.8	159.4
$\theta_{Fe-O-Fe'}$	-	-	169.3	178.8	179.2	179.5
$\theta_{N1'-Fe'-N3'}$	-	-	159.7	159.8	176.5	171.2

Table 2. Calculated parameters (bond length R in Å, bond angle θ in deg). Atom labels from fig.3, atoms of upper PcFe are denoted with '.

104 An analogous picture is given for the doubly oxidized PcFe-dimer (d,f). Two isomeres have been obtained,
 105 but both with a nearly linear bonding along the Fe–O–Fe'–O' axis. Between structure (e) to (f) only minor
 106 changes in several bond lengths can be noticed. Dimer (d) instead shows significant modifications and result
 107 in a flat upper plane, similar to (a), induced by the additional ligand.

108 5. Conclusion

109 The catalyzed [PcFe]⁺ has been observed for the first time in gas phase using MALDI and LDI. Theoret-
 110 ical calculations have shown, that the minimal energy μ -oxo bridged dimer results in two different conform-
 111 ers. The oxygen has a strong influence on the central metal atom, but leads only to minor displacements in
 112 the atomic arrangement of the phthalocyanines. However, further calculations on a higher level of theory are
 113 necessary to estimate more accurate structural parameters. Although the gas-phase basicities are adequate,
 114 a protonation of [PcFe] in MALDI seems to be unfavored.

115 References

- 116 [1] C. M. Allen, W. M. Sharman, J. E. van Lier, Current status of phthalocyanines in the photodynamic therapy of cancer, *J. Por-*
 117 *phyrins Phthalocyanines* 5 (2001) 161–169.
- 118 [2] R. Wagner, J. Lindsey, J. Seth, V. Palaniappan, D. Bocian, Molecular optoelectronic gates, *J. Am. Chem. Soc.* 118 (1996) 3996–
 119 3997.
- 120 [3] H. Moons, L. L. apok, A. Loas, S. van Doorslaer, S. M. Gorun, Synthesis, x-ray structure, magnetic resonance, and dft analysis
 121 of a soluble copper(ii) phthalocyanine lacking c-h bonds, *Inorg. Chem.* 49 (2010) 8779–8789.
- 122 [4] E. H. Yu, S. Cheng, B. E. Logan, K. Scott, Electrochemical reduction of oxygen with iron phthalocyanine in neutral media, *J.*
 123 *Appl. Electrochem.* 39 (2009) 705–711.
- 124 [5] P. Liljeroth, J. Repp, G. Meyer, Current-induced hydrogen tautomerization and conductance switching of naphthalocyanine
 125 molecules, *Science* 317 (2007) 1203–1206.
- 126 [6] D. Dini, H. Hanack, Phthalocyanines as materials for advanced technologies: some examples, *J. Porphyrins Phthalocyanines* 8
 127 (2004) 915–933.
- 128 [7] V. I. Nemykin, V. Y. Cherni, S. V. Volkov, N. I. Bundina, O. L. Kaliya, V. D. Li, E. A. Luckyantes, Further studies on the oxidation
 129 state of iron in μ -oxo dimeric phthalocyanine complexes, *J. Porphyrins Phthalocyanines* 3 (1999) 87–98.
- 130 [8] A. A. Tanaka, C. Fierro, D. Scherson, E. B. Yeager, Electrocatalytic Aspects of Iron Phthalocyanine and Its μ -Oxo Derivatives
 131 Dispersed on High Surface Area Carbon, *J. Phys. Chem.* 91 (1987) 3799–3807.
- 132 [9] J. Wichmann, C. Lupulescu, L. Wöste, A. Lindinger, Matrix-assisted laser desorption/ionization by using femtosecond laser
 133 pulses in the near-infrared wavelength regime, *Rapid Commun. Mass Spectrom.* 23 (2009) 1105–1108.
- 134 [10] M. Dewar, E. Zebisch, E. Healy, J. Stewart, AM1: A new general purpose quantum mechanical model, *J. Am. Chem. Soc.* 107
 135 (1985) 3902–3909.
- 136 [11] J. J. P. Stewart, MOPAC, Stewart Computational Chemistry, Fujitsu Ltd. 2001.
- 137 [12] F. Neese, The orca program system, *Wiley Interdisciplinary Reviews: Computational Molecular Science* 2 (1) (2012) 73–78,
 138 (Version 3.0).
- 139 [13] A. D. Becke, Density-functional thermochemistry. iii. the role of exact exchange, *J. Chem. Phys.* 98 (1993) 5648–5652.
- 140 [14] P. J. Stephens, F. J. Devlin, C. F. Chabalowski, M. J. Frisch, Ab initio calculation of vibrational absorption and circular dichroism
 141 spectra using density functional force fields, *J. Phys. Chem.* 98 (1994) 11623–11627.
- 142 [15] A. Schäfer, H. Horn, R. Ahlrichs, Fully optimized contracted Gaussian-basis sets for atoms Li to Kr, *J. Chem. Phys.* 97 (1992)
 143 2571–2577.
- 144 [16] D. A. Dixon, J. L. Gole, A. Komornicki, Absolute proton affinities of lithium dimer, sodium dimer, lithium hydride, and sodium
 145 hydride, *J. Phys. Chem.* 92 (8) (1988) 2134–2136.
- 146 [17] M.-S. Liao, S. Scheiner, Electronic structure and bonding in metal phthalocyanines, metal=fe, co, ni, cu, zn, mg, *J. Chem. Phys.*
 147 114 (22) (2001) 9780–9791.
- 148 [18] M. Sumimoto, Y. Kawashima, K. Hori, H. Fujimoto, Theoretical investigation of the molecular and electronic structures and
 149 excitation spectra of iron phthalocyanine and its derivatives, fepc and fepcl_n (l = py, cn⁻; n = 1, 2), *Dalton Trans.* (2009) 5737–
 150 5746.
- 151 [19] N. Mekhryakova, T. Gulina, V. Yu, N. Bundina, O. Kaliya, E. Luk'yanyets, Reaction of Iron Phthalocyanine with Oxygen: Critical
 152 Survey and New Data on the Structure of the Forming PcFe(II) μ -Oxo Dimer, *Russ. J. Gen. Chem.* 71 (2001) 570–590.
- 153 [20] M. Lausmann, I. Zimmer, J. Lex, H. Lueken, K. Wieghardt, E. Vogel, μ -oxodiron(iii) complexes of porphycenes", *Angew. Chem.*
 154 *Int. Ed. Engl.* 33 (7) (1994) 736–739.
- 155 [21] C. Ercolani, F. Monacelli, S. Dzugan, V. L. Goedken, G. Pennesi, G. Rossi, X-ray crystal structure of [small micro]-oxo-bis[(1-
 156 methylimidazole)-phthalocyaninatoiron(iii)] and comments on the molecular structure and chemistry of oxo-bridged iron ph-
 157 thalocyaninate dimers, *J. Chem. Soc., Dalton Trans.* (1991) 1309–1315.

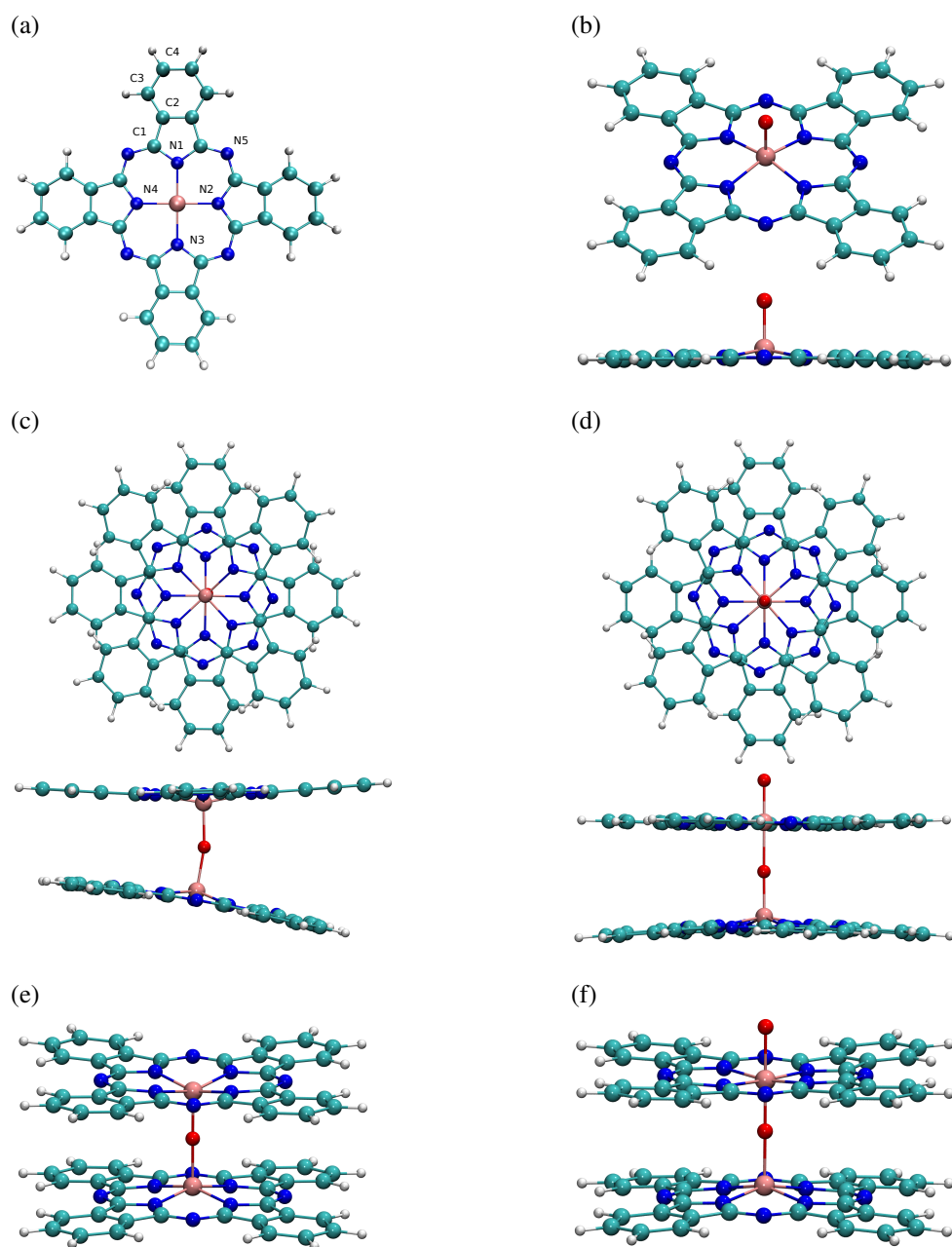


Fig. 3. Geometry optimized structures of minimal energy in tilted top and side view of (a) Iron(II)-Phthalocyanine, (b) PcFe-O, (c,e) dimer structure PcFe-O-PcFe, (d,f) doubly oxidized dimer structure PcFe-O-PcFe-O. For details see text.